論文 / 著書情報
Article / Book Information

論題(和文)	
Title(English)	Ionic Concentration Profiles by Field-Assisted Ion Exchange in Mixed Alkali Glass and Its Mechanical Reliability
著者(和文)	黒木有一, 植木, 菅原恒彦, 矢野哲司, 李在高, 船曳富士, 柴田 修一
Authors(English)	Yuichi Kuroki, Mikio Ueki, Tsunehiko Sugawara, Eiji Ichimura, Tetsuji Yano, Jaeho Lee, Fuji Funabiki, Shuichi Shibata
出典(和文)	, Vol. , No. , pp. O-07-002
Citation(English)	XX International Congress on Glass, Kyoto, Japan, Vol. , No. , pp. O-07-002
発行日 / Pub. date	2004,

IONIC CONCENTRATION PROFILES BY FIELD-ASSISTED ION EXCHANGE IN MIXED ALKALI GLASS AND ITS MECHANICAL RELIABILITY

Yuichi Kuroki, Mikio Ueki, & Tsunehiko Sugawara
Display Company, Asahi Glass Co., Ltd.,
1-12-1, Yurakucho, Chiyoda-ku, Tokyo 100-8405, Japan

Eiji Ichikura*
Research Center, Asahi Glass Co., Ltd.,
1150, Hazawa-cho, Kanagawa-ku, Yokohama 221-8755, Japan
eiji-ichikura@agc.co.jp

Tetsuji Yano, Jaeho Lee, Fuji Funabiki & Shuichi Shibata
Department of Chemistry and Materials Science, Tokyo Institute of Technology, Ookayama, Meguro-ku, Tokyo 152-8552, Japan

Field-assisted chemical tempering has proven effective in clarifying the relationship between the concentration profiles of potassium and sodium in the ion-exchange layer, and the alkali ratio of the mother glass of the system SiO_2-PbO-Al_2O_3-CaO-MgO-Na_2O-K_2O. With regard to the potassium concentration profile, it tends to change from a step-functional pattern at an alkali ratio of 57% or more to an exponential pattern at an alkali ratio of 36% or less. So as to attain an enough high reliability, a step functional pattern of the potassium concentration profile and an ion-exchange depth of 50 μm or more are both necessary.
(Key words: field-assisted ion exchange, mixed alkali glass, ionic concentration profile, biaxial bending test, and reliability)

1. Introduction

In general, some mixed alkali glasses are used as glass substrates for CRTs or flat panel displays such as PDP and FED based on bilateral requirements: one requirement that displays can retain high optical quality for a long term and one requirement that the electrical elements and circuits on the glass are functional. The former is necessary to restrict the movement of monovalent ions in glass so that it can minimize browning phenomenon caused by irradiating electron beam or ultraviolet ray. The latter is required that the amounts of K_2O and Na_2O are roughly balanced to get the mixed alkali effect (**MAE**) on the electrical resistance. On the other hand, in spite of strong market demand for lightweight glass, there is a limitation to strengthening by changing the composition of the mixed alkali glass. However, a chemical tempering by thermal diffusion is not effective for the mixed glasses because of the insufficiency of an ion-exchanged depth.[1)] For this reason, currently, a field-assisted chemical tempering method which can create a deeper ion-exchange layer within a shorter exchange time compared to that of the thermal diffusion, has been devised.[2)] However, it has not been investigated whether the composition range which can produce the **MAE** on the above characteristics corresponds with that of a field-assisted chemical tempering effect. Consequently, we studied ionic concentration profiles in ion-exchange layers in mixed alkali glass by experimenting with different alkaline oxide ratios [$Na_2O/(Na_2O+K_2O)$]; clarifying the relationship between the depth of ion-exchange layer and potassium concentration profile, and measuring the mechanical reliability by a biaxial bending test with abrasion.

2. Potassium and Sodium Concentration Profiles

For the field-assisted ion exchange experiment, we created different alkali ratio models based on a mixed alkali glass of the system SiO_2-PbO-Al_2O_3-CaO-MgO-Na_2O-K_2O for CRTs as shown in Table 1. For details regarding chemical tempering apparatus, please refer to the paper by T. Yano. [3)]

Table 1. Composition and properties of each model glass.

Model Glass	A	B	C	D	E
SiO_2	66 (mol%)				
PbO	8				
Al_2O_3	3.5				
CaO	5				
MgO	3.5				
Na_2O	14	11	8	5	3
K_2O	0	3	6	9	11
Alkali Ratio $[Na_2O/(Na_2O+K_2O)]$（%）	100	79	57	36	21
Strain Point（℃）	455	442	447	461	473
Electrical conductivity (S/cm)	2.0×10^{-5}	1.9×10^{-6}	5.4×10^{-7}	4.4×10^{-7}	4.6×10^{-7}
Depth of the ion-exchange layer (μm)	80	120	140	160	95
Surface Compression (MPa)	326	336	345	247	235

After introducing an ion-exchange layer into each sample, it was cut, and then the cross-section surface of the sample was finished with a mirror surface. The concentration profiles of potassium and sodium formed in the vicinity of the anode were measured by the EPMA (Electron Probe Micro Analyzer). Fig. 1 shows typical potassium concentration profiles of the model C glass by using a thermal diffusion method for 24 hours and a field-assisted method for 6 hours at the strain point. Given that the depth of the ion-exchange layer was the distance from the surface to the point of bulk concentration, for the sample by the field-assisted method, the depth of the ion-exchange layer was 120 μm while that for the sample by thermal diffusion was 60 μm. Accordingly, the field-assisted ion exchange could produce a deeper ion-exchange layer about twice that of the thermal diffusion method within a shorter time. In addition, a typical shape of the potassium concentration profile for the sample by the field-assisted method was not exponential but step-functional.

So as to clarify the relationship between the depth of the ion-exchange layer and the alkali ratio of the mother glass, the field-assisted ion exchange procedure was implemented at 25 ℃ below the strain point of each model glass as shown in Table 1. Then we measured the average depth of the ion-exchange layer by back-scattered electron imaging. As shown in Fig. 2, the average depth of the ion-exchange layer rises to the maximum at an alkali ratio of 36% and then, decreases with increasing alkali ratio. The least depth is achieved at an alkali ratio of 100%, that is, potassium free. Thus, it was found that there is a roughly inverse relationship between the depth of the ion-exchange layer and the electrical conductivity of the mother glass for a given alkali ratio range. In other words, the degree of the electrical conductivity cannot account for the depth of the ion-exchange layer.

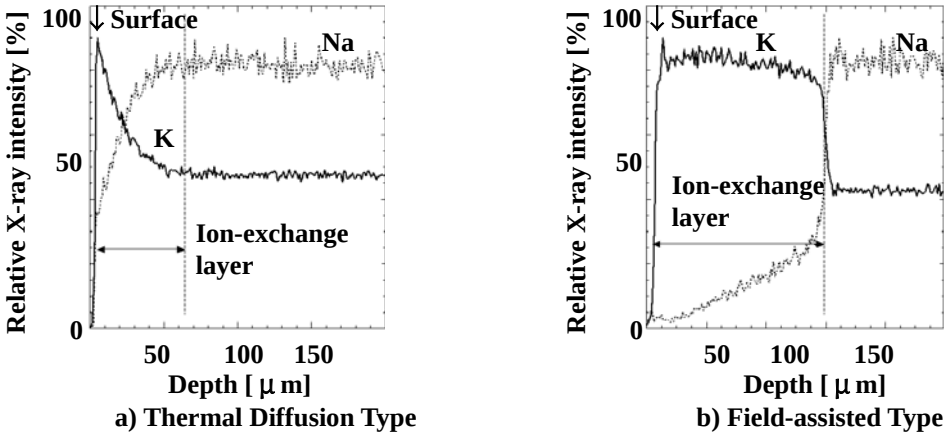

Fig. 1. Typical potassium and sodium concentration profiles in ion-exchange layer by thermal diffusion and field-assisted chemical tempering.

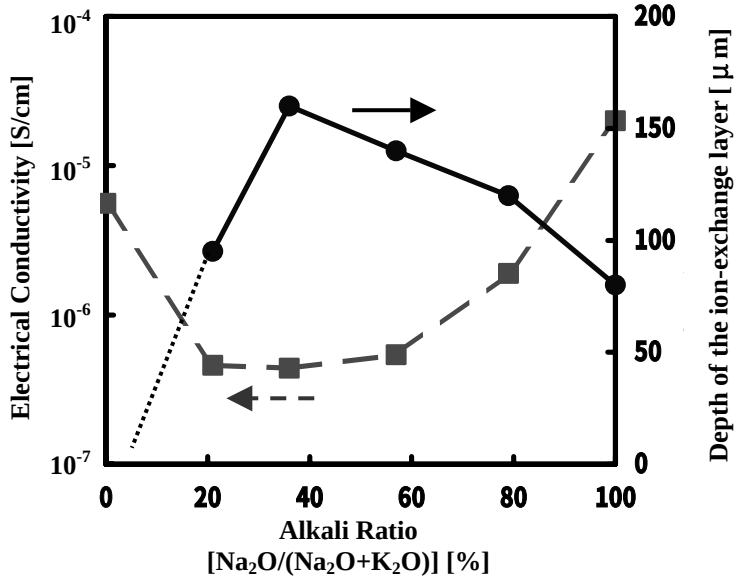

Fig. 2. Electric conductivity and Depth of ion-exchange layer vs. Alkali ratio in the initial glass.

Next, we outlined a comparative chart of potassium and sodium concentration profiles formed near the anode in Fig. 3. With regard to the potassium concentration profile, it tends to change from a step-functional pattern at an alkali ratio of 57% or more to an exponential pattern at an alkali ratio of 36% or less. Thus it is considered that the alkali ratio of 36% used in the model D glass marks the inflection point of the mixed alkali glass. On the other hand, it was found that sodium concentration profiles of all the five samples show an increase from the surface to the boundary between the ion-exchange layer and the mother glass, and that the profile at an alkali ratio of 57% or more shows a sudden change at the boundary, whereas that at an alkali ratio of 36% or less shows only a gradual change. In studying these results, it is our understanding that the transport numbers should be taken into account, since the transport numbers of Na and K ion both display sudden changes around this alkali ratio, at which the mother glass showed the minimum value of electrical conductivity, as reported by T. Yano.[3)]

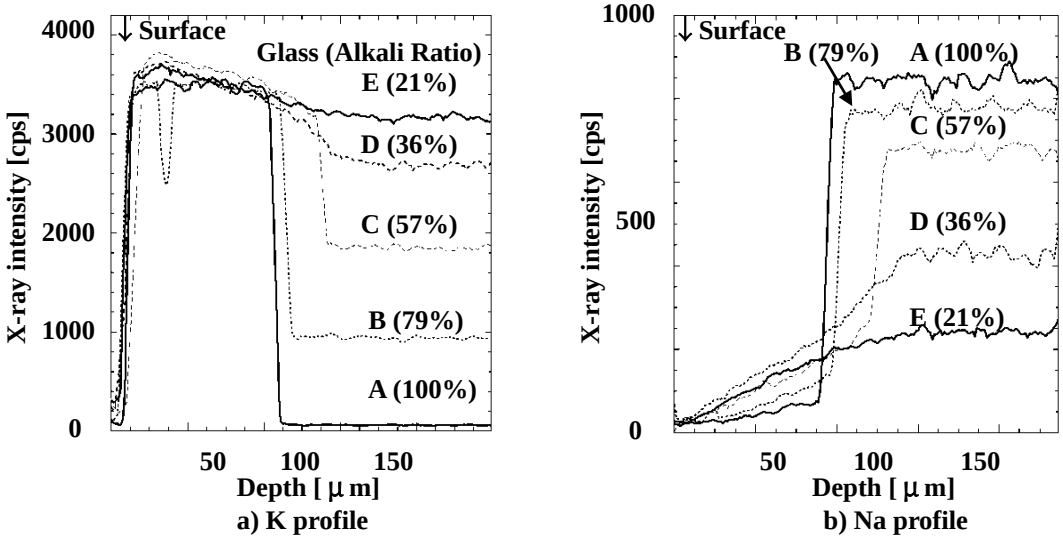

Fig. 3. Comparative chart of potassium and sodium concentration in the model glasses.

In addition, the total amount of two different alkali ions in the direction of the depth in the ion-exchange layer was quantitatively evaluated using EPMA. As shown in Fig. 4, it can easily be seen that total amount of alkali at each point in the layer increases with increasing distance from the

surface. It can be also understood that the total volume of the two alkali ions in the exchanged layer in each sample decreases compared to that in each mother glass, and that there is a dependency of the decreased volume on the alkali ratio. The meshed area indicates the decreased volume of two alkali ions at an alkali ratio of 79%. It is comparable to approx. 14% of the total volume of alkali ions in the exchanged layer. Moreover, it was indicated that the movement of non-bridged oxygen ions to the anode should be taken into account, since there was a decrease of oxygen ions in the layer, in quantitatively analyzing the surface of a model glass by EPMA and XPS (X-ray Photoelectron Spectroscopy). It is our understanding of these facts that there is a mechanism which prevents the movement of potassium ions to the cathode.

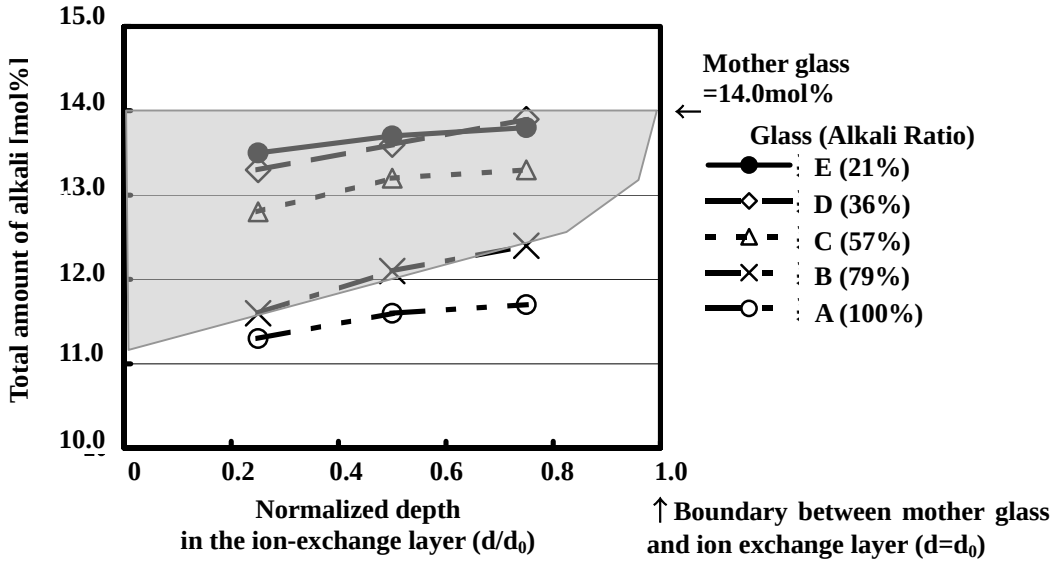

Fig. 4. The total amount of the alkali ions vs. Normalized depth in the ion-exchange layer.

3. Mechanical Reliability of Field-Assisted Chemical Tempering Glass

The objective of the field-assisted chemical tempering is to generate a high degree of strengthening with deeper compression layer to be able to overcome the surface flaws and enhance the reliability for the delayed breakage. Therefore, we measured the abraded strength as a function of the depth of ion-exchange layer. In the beginning of the experiment, glass discs of 70mm diameter and 3mm thickness were prepared from the model C glass. After that, either of two kinds of chemical tempering procedures was implemented on a 55mm diameter area at the center of each glass disc at the strain point(see Table 1). Prior to the test, every glass disc was abraded with 150-J abrasion under a constant loading of 8MPa at the middle portion of the lower surface, using a ring-on-ring fixture as shown in Fig. 5. Such sample preparations were made assuming that a CRT is under constant load due to the state of evacuation and that flaws may generate after evacuating. The discs were tested in biaxial bending using the above fixture on a 50mm diameter ring and a 12mm diameter loading piston at the center. The loading speed was 1mm per minute.

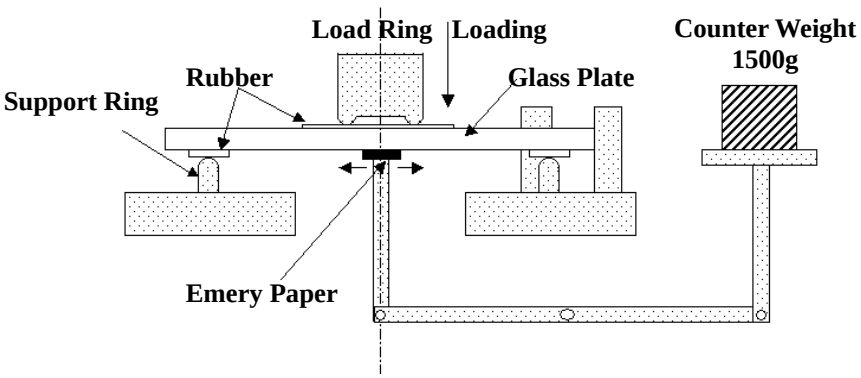

Fig. 5. Schematic figure of biaxial bending and abrasion method.

Fig. 6 shows the Weibull plot of the abraded strength data for three kinds of field-assisted tempering samples of the model C glass which have the ion-exchange depth of 30, 50 and 70 μm, respectively, in comparison to those of a non-tempered sample and a conventional chemical-tempered sample. The abraded strength data of all the field-assisted chemical tempering samples are considerably higher than that of the conventional chemical-tempered sample. The parallel shift of Weibull distribution on the samples of 50 μm and 70 μm from that of the non-tempered samples is indicative of being highly reliable.

Furthermore, we investigated the difference between the mechanical reliability of the step functional pattern and that of the exponential pattern of potassium concentration profile in the ion-exchange layer. The glass discs of 50mm diameter and 3 mm thickness were prepared from the model A glass with the alkali ratio of 100% and the model D glass with the alkali ratio of 36%. The field-assisted chemical tempering procedure was implemented on a 35mm diameter area at the center of each glass disc at 10 ℃ below the strain point of each model glass. The compressive stresses of the model A and D glass were 84MPa and 62MPa, respectively. The discs were tested in biaxial bending using the fixture on a 30mm diameter ring and a 10mm diameter loading-piston at the center. Fig. 7 shows the Weibull plot of biaxial strength data for two kinds of samples of the models A and D glass. The average strength and the shape parameter of the model A glass were both significantly higher than those of the model D glass. From these results, it can easily be understood that, in order to attain a high reliability for the field-assisted chemical tempering, a step functional pattern of potassium concentration profile and an ion-exchange depth of 50 μm or more are both necessary.

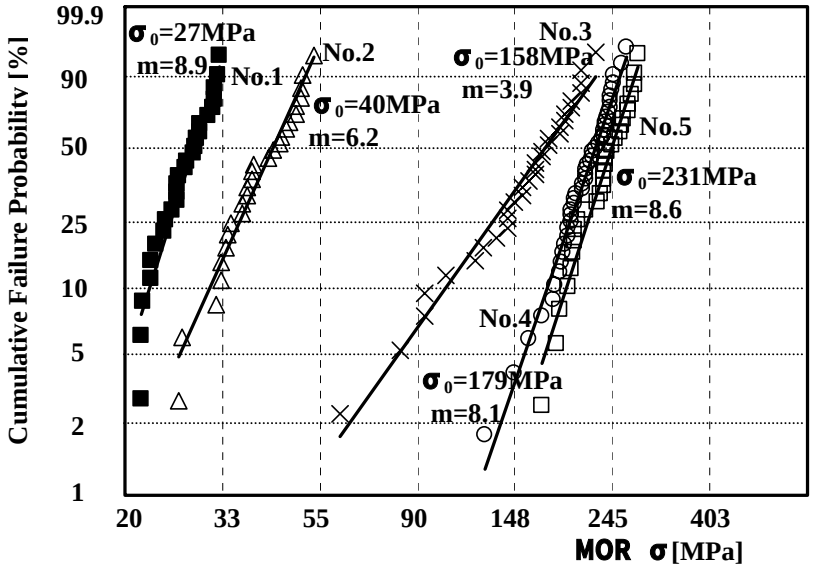

No.1; Non Tempered Glass
No.2; Tempered Glass by Thermal Diffusion Method
No.3; Field-assisted Tempering Glass of 30 μm ion exchange depth
No.4; Field-assisted Tempering Glass of 50 μm ion exchange depth
No.5; Field-assisted Tempering Glass of 70 μm ion exchange depth

Fig. 6. Weibull prot of the abraded strength of the model C glass by biaxial bending.

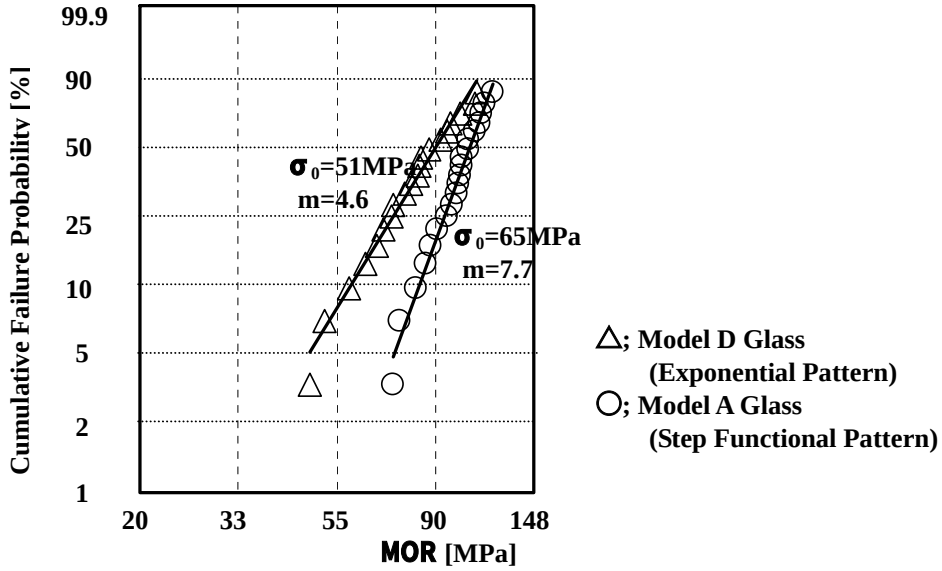

Fig. 7. Weibull plot of the abraded strength of two different mixed alkali glasses by biaxial bending.

4. Conclusion

Field-assisted chemical tempering has proven effective in clarifying the relationship between the concentration profiles of potassium and sodium in the ion-exchange layer, and the alkali ratio of the mother glass. It was carried out in mixed alkali glasses of the system SiO_2-PbO-Al_2O_3-CaO-MgO-Na_2O-K_2O with different alkaline oxide ratios [Na_2O/ (Na_2O+K_2O)]. With regard to the potassium concentration profile, it tends to change from a step-functional pattern at an alkali ratio of 57% or more to an exponential pattern at an alkali ratio of 36% or less. So as to attain a high reliability for the field-assisted chemical tempering, a step functional pattern of the potassium concentration profile and an ion-exchange depth of 50 μm or more are both necessary. On the other hand, the range of alkali ratio from 36% to 57% is suitable for attaining good **MAE** on the electrical resistance. Consequently, the composition range that can produce the **MAE** on the above characteristic and can get the effectiveness of field-assisted chemical tempering would be comparatively narrow around an alkali ratio of 57%.

5. Acknowledgements

The authors are grateful to Emeritus Professor M. Yamane of Tokyo Institute of Technology for his valuable advice on this study.

6. Reference

1) T. Sugawara and T. Murakami, J. SID, **11**, 133-138(2003).
2) T. Sugawara, M. Ueki, Y. Kuroki, T. Murakami, N. Shimizu, and M. Segawa, SID'03 Digest, 154-157(2003).
3) T. Yano, J. Lee, F. Funabiki, S. Shibata, E. Ichikura, Y. Kuroki, M. Ueki and T. Sugawara, appeared in this volume.